VISION-BASED LATERAL CONTROL OF VEHICLES

J. Košecká, R. Blasi, C. J. Taylor and J. Malik
Department of Electrical Engineering and Computer Sciences
University of California at Berkeley
Berkeley, CA 947, USA.
email: janak,blasirs,camillo,malik@cs.berkeley.edu

Keywords: lateral control, computer vision, autonomous systems

ABSTRACT

We describe the problem of automated steering using computer vision, focusing the analysis and design on appropriate lateral controllers. We investigate various static feedback strategies where the measurements obtained from vision, namely offset from the centerline at some lookahead distance and the angle between the road tangent and the orientation of the vehicle at some lookahead distance, are directly used for control. Within this setting we explore the role of lookahead, its relation to the vision processing delay, the longitudinal velocity and road geometry. Results from ongoing experiments with our autonomous vehicle system are presented along with simulation results.

INTRODUCTION

This paper addresses the problem of designing control systems for steering a motor vehicle along a highway using the output from a video camera mounted inside the vehicle. Several aspects of this problem have been examined extensively in the past, both in the psychophysics literature [7] as well as in control theoretic studies. In the kinematic setting there have been several attempts to formulate the vision-based steering task in the image plane [11], [3]. A stability analysis was provided for an omnidirectional mobile base trying to align itself with a straight road [3] or nonholonomic mobile base following an arbitrary ground analytic curve [8]. The controllers designed based on kinematic models were either tested in simulation or in experiments at speeds below 20 m/s. However at higher speeds dynamic effects are quite pertinent and the need for a dynamic model becomes apparent.

The control problem in a dynamic setting, using measurements ahead of the vehicle, has been explored by [9] who proposed a constant control law proportional to the offset from the centerline at a look-ahead distance. Their analysis showed that closed loop stability for this controller can always be obtained by increasing the look-ahead distance to an appropriate value. Dickmanns, et al [2] developed a Kalman-filter based observer which estimated the state of the vehicle with respect to the road along with the road geometry and used the estimate for full state feedback using a pole-placement method. Further studies typically use a small and fixed look-ahead distance and the control objective is formulated either at the look-ahead distance [5] or at the center of gravity of the vehicle [10]. An analysis of the tradeoffs between the performance requirements and robustness of the system can be found in [5].

This paper will discuss the problem of automated steering using computer vision, focusing on the analysis of the problem and controller design choice. We propose a static feedback strategy where the measurements obtained from vision, namely offset from the centerline and angle between the road tangent and the orientation of the vehicle at some look-ahead distance, are directly used for control. Within this setting we explore the role of lookahead, its relation to the vision processing delay, longitudinal velocity and road geometry.

MODELING

The dynamics of the vehicle can be described by a detailed 6-DOF nonlinear model [10]. Since it is possible to decouple the longitudinal and lateral dynamics, a linearized model of the lateral vehicle dynamics is used for controller design. The linearized model of the vehicle retains only lateral and yaw dynamics, assumes small steering angles and a linear tire model, and is parameterized by the current longitudinal velocity. Coupling the two front wheels and two rear wheels together, the resulting bicycle model (Figure 1) is described by the following variables and parameters:

$\boldsymbol{v}$ linear velocity vector (v_x, v_y), v_x denotes speed
α_f, α_r side slip angles of the front and rear tires
ψ vehicle yaw angle within a fixed inertial frame
δ_f front wheel steering angle
δ commanded steering angle
m total mass of the vehicle
I_ψ total inertia vehicle around center of gravity (CG)
l_f, l_r distance of the front and rear axles from the CG
l distance between the front and the rear axle $l_f + l_r$
c_f, c_r cornering stiffness of the front and rear tires.

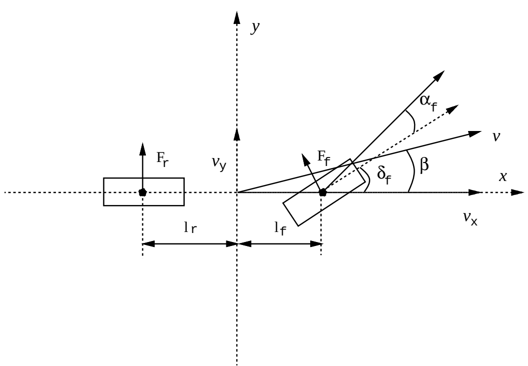

Fig. 1. The motion of the vehicle is characterized by its velocity $\boldsymbol{v} = (v_x, v_y)$ expressed in the vehicle's inertial frame of reference and its yaw rate $\dot{\psi}$. The forces acting on the front and rear wheels are F_f and F_r, respectively.

Parameters for the Honda Accord used in our experiments were m = 1590 kg, I_ψ = 2920 kg m^2, l_f = 1.22 m, l_r = 1.62 m, $c_f = c_r$ = 2 x 60000 N/rad. The cornering stiffness is increased by factor 2 since the two tires are lumped together.

The lateral dynamics equations are obtained by computing the net lateral force and torque acting on the vehicle following Newton-Euler equations [6] and choosing $\dot{\psi}$ and v_y, as state variables. The state equations have the following form:

$$\begin{bmatrix} \dot{v}_y \\ \ddot{\psi} \end{bmatrix} = \begin{bmatrix} -\frac{a_1}{m v_x} & \frac{-m v_x^2 + a_2}{m v_x} \\ \frac{a_3}{I_\psi v_x} & -\frac{a_4}{I_\psi v_x} \end{bmatrix} \begin{bmatrix} v_y \\ \dot{\psi} \end{bmatrix} + \begin{bmatrix} b_1 \\ b_2 \end{bmatrix} \delta_f \quad (1)$$

where $a_1 = c_f + c_r$, $a_2 = c_r l_r - c_f l_f$, $a_3 = -l_f c_f + l_r c_r$, $a_4 = l_f^2 c_f + l_r^2 c_r$, $b_1 = \frac{c_f}{m}$ and $b_2 = \frac{l_f c_f}{I_\psi}$.

Vision Dynamics. The additional measurements provided by the vision system (see Figure 2) are:

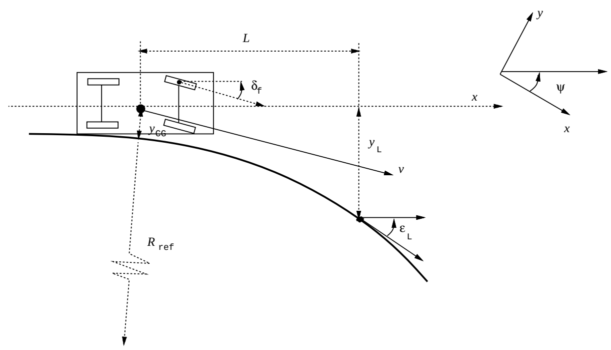

Fig. 2. The vision system estimates the offset from the centerline y_L and the angle between the road tangent and heading of the vehicle ε_L at some look-ahead distance L.

y_L the offset from the centerline at the look-ahead,
ε_L the angle between the tangent to the road and the vehicle orientation
K_L the curvature of the road at the look-ahead,

L denotes the look-ahead distance. The equations capturing the evolution of these measurements due to the motion of the car and changes in the road geometry are:

$$\dot{y}_L = v_x\, \varepsilon_L - v_y - \dot{\psi} L \quad (2)$$

$$\dot{\varepsilon}_L = v_x\, K_L - \dot{\psi} \quad (3)$$

We can combine the vehicle lateral dynamics and the vision dynamics into a single dynamical system of the form:

$$\dot{\boldsymbol{x}} = A\,\boldsymbol{x} + B\,\boldsymbol{u} + E\,\boldsymbol{w}$$
$$\boldsymbol{y} = C\,\boldsymbol{x} + D\,\boldsymbol{u} + F\,\boldsymbol{w}$$

with the state vector $\boldsymbol{x} = [v_y, \dot{\psi}, y_L, \varepsilon_L]^T$, the output $y = [\dot{\psi}, y_L, \varepsilon_L]^T$ and control input $\boldsymbol{u} = \delta_f$, disturbance $\boldsymbol{w} = K_L$ and matrices:

$$A = \begin{bmatrix} -\frac{a_1}{m v_x} & \frac{-m v_x^2 + a_2}{m v_x} & 0 & 0 \\ \frac{a_3}{I_\psi v_x} & -\frac{a_4}{I_\psi v_x} & 0 & 0 \\ -1 & -L & 0 & v_x \\ 0 & -1 & 0 & 0 \end{bmatrix} \; B = \begin{bmatrix} b_1 \\ b_2 \\ 0 \\ 0 \end{bmatrix} \; E = \begin{bmatrix} 0 \\ 0 \\ 0 \\ v_x \end{bmatrix}$$

The output equations have following form:

$$y = C\,\boldsymbol{x} \;\text{ where }\; C = \begin{bmatrix} 0 & 1 & 0 & 0 \\ 0 & 0 & 1 & 0 \\ 0 & 0 & 0 & 1 \end{bmatrix} \quad (4)$$

The road curvature K_L enters the model as an exogenous disturbance signal.

VISION SYSTEM

The vision-based lane tracking system used in our experiments is an improved version of the one presented at last year's ITS conference [12]. This system takes its input from a single forward-looking CCD video camera. It extracts potential lane markers from the input using a simple template-based scheme. It then finds the best linear fits to the left and right lane markers over a certain lookahead range through a variant of the Hough transform. From these measurements we can compute an estimate for the lateral position and orientation of the vehicle with respect to the roadway at a particular lookahead distance, L.

The vision system is implemented on an array of TMS320C40 digital signal processors which are hosted on the bus of an Intel-based industrial computer. The system processes images from the video camera at a rate of 30 frames per second. The total delay between the time the shutter on the CCD video camera is closed and the time the measurements for that image are available to the control computer is 57 milliseconds. Since the delay is quite substantial we will explicitly consider it in the controller design.

ANALYSIS

The block diagram of the overall system following the state equations is shown in Figure 3. The transfer function $V_1(s)$ between the steering angle δ_f and offset at the look-ahead y_L can be obtained by taking a Laplace transform of the state equations and has the following form:

$$V_1(s) = \frac{1}{s^2} \frac{as^2 + bs + c}{ds^2 + es + f} \tag{5}$$

where the numerator is a function of both speed and lookahead distance and the denominator is parameterized by the speed of the car. $V_1(s)$ can be rewritten according to Figure 3 by singling out the vehicle dynamics in terms of $\ddot{y}_{CG}$ and $\ddot{\psi}$ followed by the integrating action $1/s^2$:

$$V_1(s) = \frac{1}{s^2}(G(s) + L\, G_2(s)) \tag{6}$$

where $G(s)$ and $G_2(s)$ are transfer functions between steering angle and lateral acceleration and

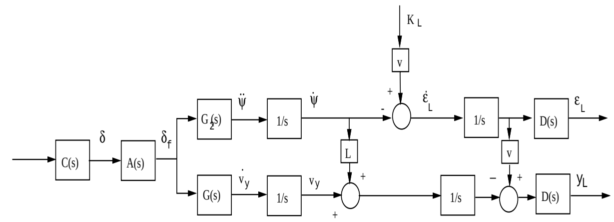

Fig. 3. The block diagram of the overall system with the two outputs provided by the vision system.

yaw acceleration respectively. There are two additional components which appear in the block diagram. The actuator $A(s)$ is modeled as a low pass filter of the commanded steering angle δ and a pure time delay element $D(s) = e^{-T_d s}$ representing the latency T_d of the vision subsystem. In our system $T_d = 0.057$ s. The transfer function $C(s)$ corresponds to the controller to be designed.

Control objective. The vehicle control objective is to follow the reference path specified by radius R_{ref} (curvature $K_{ref} = \frac{1}{R_{ref}}$). Perfect tracking of the road in steady state corresponds to the zero offset $y_{CG} = 0$ of the vehicle's center of the gravity from the centerline, with the orientation of the vehicle aligned with the tangent to the road. The speed is chosen such as not to exceed lateral acceleration of 0.3-0.4g, where g = 9.81 m/s^2, which has been shown to be comfortably accepted by humans. In addition to limits on the steady-state lateral acceleration an important design criterion is that of passenger comfort. This is typically expressed in terms of jerk, corresponding to the rate of change of acceleration. For a comfortable ride no frequency above 0.1-0.5 Hz should be amplified in the path to lateral acceleration [5]. Additional road following criteria can be specified in terms of maximal allowable offset y_{Lmax} as a response to the step change in curvature as well as bandwidth requirements on the transfer function $F(s) = \frac{y_L(s)}{K_{ref}(s)}$. Since the primary advantage of the vision system is the availability of measurements at a point ahead of the vehicle, we will analyze how the choice of the look-ahead distance L affects the transfer function $V_1(s)$ between steering angle and the offset at the look-ahead. The analysis will also take into account the processing delay T_d inherent in the vision system which substantially affects the stability of the system.

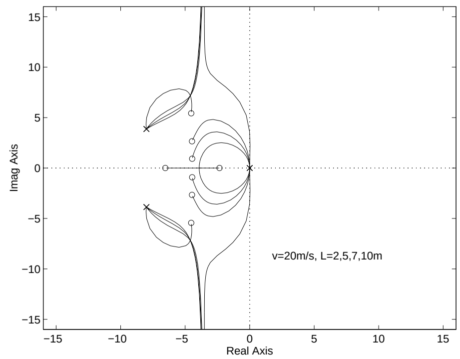

Fig. 4. Increasing the lookahead distance L moves the zeros of the transfer function $V_1(s)$ closer to the real axis, which improves their damping.

Lookahead. A root locus of the transfer function $V_1(s)$ is in Figure 4. The transfer function $V_1(s)$ has four poles and two zeros, where the damping of the zero pair affects the location of closed loop poles and subsequently the transient response of the system more profoundly. As the lookahead increases the zeros move closer to the real axis, improving the damping of the closed loop poles of $V_1(s)$. Increasing the velocity moves both poles and zeros of $V_1(s)$ towards the imaginary axis, resulting in a poor damping of the poles. The choice of proper lookahead distance is therefore important for stability and performance of the system.

Delay. Another parameter which affects the behavior of the overall system is the delay associated with the vision system. The delay element adds an additional phase lag over the whole range of frequencies having a clear destabilizing effect on the overall system and limiting the system's bandwidth. More detailed analysis can be found in [6], [1].

Controller Design. Analysis reveals that up to 15 m/s the lookahead one can guarantee satisfactory damping of the closed loop poles of $V_1(s)$ and compensate for the delay using simple unity feedback control with proportional gain in the forward loop. As the velocity increases the transient response is affected more by the poor damping of the poles of $V_1(s)$ introducing additional phase lag around the 0.1-2 Hz. Since further increasing the lookahead does not improve the damping, gain compensation only cannot achieve satisfactory performance. The natural choice for obtaining an additional phase lead in the frequency range 0.1-2 Hz would be to introduce some derivative action. In order to keep the bandwidth low an additional lag term is necessary. One satisfactory lead-lag controller has the following form:

$$C(s) = \frac{0.09s + 0.18}{0.025s^2 + 1.5s + 20} \qquad (7)$$

where $C(s)$ is a lead network in series with a single pole. The above controller was designed for a velocity of 30 m/s (108 km/h, 65 mph), a lookahead of 15 m and 60 ms delay. The resulting closed loop system has a bandwidth of 0.45 Hz with a phase lead of $45°$ at the crossover frequency. A discretized version of the above controller taking into account the 30 ms sampling time of the vision system have been used in our experiments.

Since increasing the speed has a destabilizing effect on $V_1(s)$, designing the controller for the highest intended speed guarantees stability at lower speeds and achieves satisfactory ride quality. In order to tighten the tracking performance at lower speeds individual controllers can be designed for various speed ranges and gain scheduling techniques used to interpolate between them.

The steady state behavior of the system during perfect tracking of a curve with radius R_{ref}, is characterized by particular values of $\dot{\psi}_{ref}, v_{yref}$ and δ_{ref}. By setting the $[\dot{v}_y, \ddot{\psi}, \dot{y}_L, \dot{\varepsilon}_L]^T$ to 0, the steering angle δ_{ref} can be obtained from state equations and becomes:

$$\delta_{ref} = K_{ref}\,(l - \frac{(l_f c_f - l_r c_r) v_x^2 m}{c_r c_f l})\,. \qquad (8)$$

The feedforward control law essentially provides information about the disturbance ahead of the car and improves the transient behavior of the system when encountering changes in curvature. The effectiveness of the feedforward term depends on the quality of the curvature estimates. We discuss the curvature estimation process as part of the observer design in the next section .

OBSERVER ISSUES AND DESIGN

In order to apply modern state space control techniques we require access to the states of the system. This is usually accomplished by constructing an observer. Our first step is to rewrite state equations in the following form:

$$\dot{x} = A(v_x)x + B\delta_f \qquad (9)$$

where $\boldsymbol{x} = [v_y, \dot{\psi}, y_L, \varepsilon_L, K_L]^T$ and

$$A(v_x) = \begin{bmatrix} -\frac{a_1}{mv_x} & \frac{-mv_x^2+a_2}{mv_x} & 0 & 0 & 0 \\ \frac{a_3}{I_\psi v_x} & -\frac{a_4}{I_\psi v_x} & 0 & 0 & 0 \\ -1 & -L & 0 & v_x & 0 \\ 0 & -1 & 0 & 0 & v_x \\ 0 & 0 & 0 & 0 & 0 \end{bmatrix} \quad B = \begin{bmatrix} b_1 \\ b_2 \\ 0 \\ 0 \\ 0 \end{bmatrix}$$

Note that the state vector $\boldsymbol{x}$ has been augmented with the road curvature K_L since we are interested in estimating this parameter as well. This differential equation can be converted to discrete time in the usual manner by assuming that the control input, δ_f, is constant over the sampling interval T.

$$\boldsymbol{x}(k+1) = \Phi(v_x)\boldsymbol{x}(k) + \beta\boldsymbol{u}(k) \qquad (10)$$

Equation (10) allows us to predict how the state of the system will evolve between sampling intervals. Measurements of the system state can be obtained from two sources: the vision system provides us with measurements of y_L and ε_L, while the on-board fiber optic gyro provides us with measurements of the yaw rate of the vehicle, $\dot{\psi}$. Our use of the yaw rate sensor measurements is analogous to the way in which information from the proprioceptive system is used in animate vision. Considering $\boldsymbol{y} = \left[\dot{\psi}, y_L, \varepsilon_L\right]^T$ the measurement equation for our system can be written as in Equation 4:

$$\boldsymbol{y} = C\boldsymbol{x} \qquad (11)$$

The measurement vector $\boldsymbol{y}$ is used to update an estimate for the state of the system $\hat{\boldsymbol{x}}$ as shown in the following equation:

$$\hat{\boldsymbol{x}}^+(k) = \hat{\boldsymbol{x}}^-(k) + L(\boldsymbol{y}(k) - C\hat{\boldsymbol{x}}^-(k)) \qquad (12)$$

where $\hat{\boldsymbol{x}}^-(k)$ and $\hat{\boldsymbol{x}}^+(k)$ denote the state estimate before and after the sensor update respectively.

The gain matrix L can be chosen in a number of ways [4], depending on the assumptions one makes about the availability of noise statistics and the criterion one chooses to optimize.

Experimental Results. The controller was tested both in simulation and in real experiments. In the simulation the full nonlinear model of the vehicle has been used and the design has been tested for various road scenarios (see Figure 5). The maximum offset did not exceed 10 cm and the lateral acceleration was within passenger comfort standards. The initial experiments were carried out with the actual vehicle on the stretch of California highway, with speeds varying between 20-70 mph.

With the introduction of the lead-lag controller and an observer to filter noise from our measurements, we were able to take our experimental vehicle to speeds of 90 mph for extended periods of time without any degradation in passenger comfort. The lateral controller has been subsequently integrated into a system with a velocity controller, obstacle de-

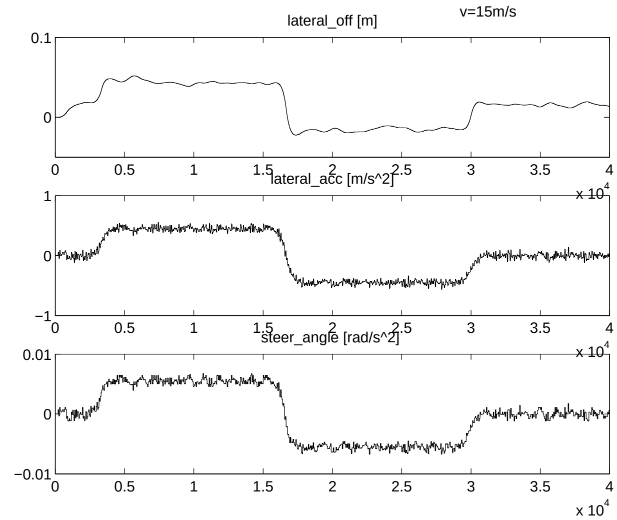

Fig. 5. Tracking changes in curvature without intermediate straight line segments for various velocities. Reference path with straight line segment, followed by two curved segments with K_{1ref} = 0.002 m^{-1} and K_{2ref} = -0.002m^{-1} is followed at v = 15m/s.

Fig. 6. Camera's view of the Honda Accord used in experiments

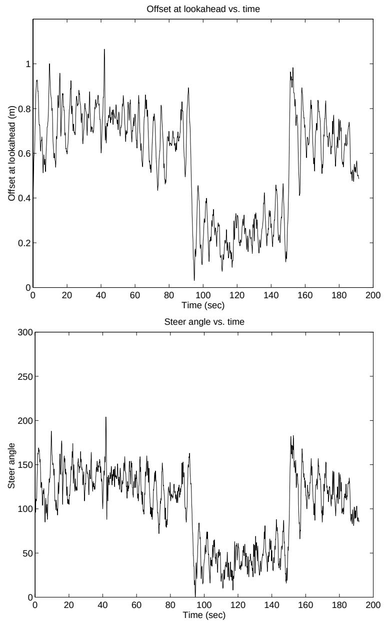

Fig. 7. (a) The offset at the lookahead y_L used for control purposes. (b) Commanded steering angle.

tection and avoidance system, and an intra-vehicle communication system.

CONCLUSIONS

The main focus of this analysis was on the role of the look-ahead and the delay in the design of a steering controller. The delay plays an important role in the system and should be taken into account explicitly in case of output feedback strategies, such as the ones we presented. We showed that sufficiently large look-ahead and appropriate choice of gain can compensate for the additional phase lag introduced by delay and vehicle dynamics at lower velocities. At higher velocities additional lead action was introduced in order to achieve desired phase margin. Since the criteria for passenger comfort put quite stringent limits on the bandwidth of the system an additional pole (lag) was necessary in order to keep the low bandwidth.

The resulting controller has been tested both in simulation and experiments. Further experiments for different road scenarios and detailed performance evaluation of the experimental testbed are currently being performed.

Introducing a real-time observer process into the system not only reduces the noise inherent in the system's sensor measurements, but also provides an accurate estimate of the current vehicle state, circumventing the delay in the vision system and permitting the implementation of more advanced state-space based controllers.

Acknowledgment. This research has been supported by Honda R&D North America Inc., Honda R&D Company Limited, Japan, ITS MOU257 and MURI program DAAH04-96-1-0341.

REFERENCES

[1] R. S. Blasi. A study of lateral controllers for the stereo drive project. Master's thesis, Department of Computer Science, University of California at Berkeley, 1997.

[2] E. D. Dickmans and B. D. Mysliwetz. Recursive 3-D road and relative ego-state estimation. *IEEE Transactions on PAMI*, 14(2):199–213, February 1992.

[3] B. Espiau, F. Chaumette, and P. Rives. A new approach to visual servoing in robotics. *IEEE Transactions on Robotics and Automation*, 8(3):313 – 326, June 1992.

[4] Arthur Gelb *et al. Applied optimal estimation*. MIT Press, 1994.

[5] J. Guldner, H.-S. Tan, and S. Patwarddhan. Analysis of automated steering control for highway vehicles with look-down lateral reference systems. *Vehicle System Dynamics (to appear)*, 1996.

[6] J. Košecká. Vision-based lateral control of vehicles:look-ahead and delay issues. Internal Memo, Department of EECS, University of California Berkeley, 1997.

[7] M. F. Land and D. N. Lee. Where we look when we steer? *Nature*, 369(30), June 1994.

[8] Y. Ma, J. Košecká, and S. Sastry. Vision guided navigation for a nonholonomic mobile robot. In *submitted to CDC'98*, 1997.

[9] Ü. Özgüner, K. A. Ünyelioglu, and C. Hatipoğlu. An analytical study of vehicle steering control. In *Proceedings of the 4th IEEE Conference on Control Applications*, pages 125 – 130, 1995.

[10] H. Peng. *Vehicle Lateral Control for Highway Automation*. PhD thesis, Department of Mechanical Engineering, University of California, Berkeley, 1992.

[11] D. Raviv and M. Herman. A 'non-reconstruction' approach for road following. In *SPIE proceedings on Intelligent Robots and Computer Vision*, pages 2–12, 1991.

[12] C. J. Taylor, J. Malik, and J. Weber. A real-time approach to stereopsis and lane-finding. In *Proceedings of the 1996 IEEE Intelligent Vehicles Symposium*, pages 207–213, Seikei University, Tokyo, Japan, September 19-20 1996.